OPEN ACCESS Freely available online

Journal of Aeronautics & Aerospace Engineering

Review Article

Small Object Detection Capabilities Enabled by Employing sUAS Integrated with Modern Sensors

Oleg A Yakimenko*

Department of Systems Engineering, Naval Postgraduate School, California, United States Of America

ABSTRACT

Manned aircraft have been widely used to detect objects/anomalies on the ground using daytime and nighttime sensors. The introduction and development of Unmanned Aerial Systems (UAS) allowed transitioning of this dull and often dirty and dangerous task on to them. Further development and miniaturization of UAS and their sensors provide these small UAS (sUAS) with almost the same capabilities as those of the larger drones. Indeed, the flight duration and potential coverage of sUAS are much more modest compared to the larger systems. However, an opportunity to fly at very low altitudes creates a unique niche. This paper presents a brief summary of recent research activities conducted to explore feasibility of several new applications of sUAS equipped with modern small single-spectrum and multi-spectral sensors to detect and possibly classify relatively small (down to several centimeters) objects. The goal of the paper is to encourage further exploration of these and other promising applications for a growing fleet of small robotic aircraft.

Keywords: Unmanned Aerial System (UAS); Aerial imagery; Object detection and classification; Multi-Spectral (MS) sensor; Machine Learning (ML)

INTRODUCTION

For the past two decades, Unmanned Aerial Systems (UAS) have primarily been used for Intelligence, Surveillance, and Reconnaissance (ISR) missions at different levels – from small tactical Group 1 and 2 UAS (like RQ-14, RQ-11, Insitu ScanEagle) supporting special operation force teams at the tactical level all way up to large Group 5 UAS (like MQ-9 and RQ-4) supporting ISR operations at the strategic level. The latest local armed conflicts revealed yet another niche for UAS to be used as a loitering munition (aka suicide drone, kamikaze drone, expendable UAS, or exploding drone). The effectiveness of using UAS in any of these two applications relies on modern high-resolution daytime Electro-Optical (EO) and nighttime Infra-Red (IR) sensors.

These days, a typical EO/IR sensor provides resolution (the number of pixels that a camera can capture in each frame) of at least 1,920 pix by 1,080 pix (e.g., L3Harris WEBCAM MS series sensors) [1] and a variable Field of View (FoV) (focal length), which enables detection and tracking of relatively small objects. Depending on the flying Above Ground Level (AGL) altitude, these sensors assure spatial resolution of about 3 cm/pix. Miniaturized EO/IR sensors integrated with smaller, commercially available drones feature the same in not even better resolution and because they can fly at a much lower altitude compared to a pattern altitude of a typical ISR or suicide mission, such a platform enables superb spatial resolution opening the door to novel applications. For example, Sony RX1 RII camera flyable on many small UAS (sUAS) to include Quantum Systems Trinity 90+ fixed-wing eVTOL platform features 7,952 pix by 5,304 pix resolution and DJI Zenmuse X7 camera flyable on many multirotor sUAS to include DJI drones features a 6K (6,016 pix by 3,200 pix) video capability. In addition to this, sUAS can carry other commercially-available advanced sensors like LiDARs and Multi-Spectral (MS) sensors [2].

This paper reviews several recent attempts by the research team led by the author to explore feasibility of using these modern tools for several novel applications. The first example deals with using multiple (swarm) sUAS equipped with EO sensor to detect foreign object debris on a runway. Next, a brief description of research concerned with detection of unexploded ordnance using Machine Learning (ML) is provided. To improve the detection rate, instead of a common EO sensor a sUAS used in this latter research was equipped with a miniaturized MS sensor. Fusing the detection results from multiple spectra resulted in a superb detection capability as opposed to an EO sensor. The subsequent section shows an example of using sUAS and EO sensor not only to detect

Correspondence to: Oleg A Yakimenko, Department of Systems Engineering, Naval Postgraduate School, California, United States of America, E-mail: oayakime@nps.edu

Received: 29-Dec-2023, Manuscript No. JAAE-23-28794; **Editor assigned:** 02-Jan-2024, PreQC No. JAAE-23-28794 (PQ); **Reviewed:** 16-Jan-2024, QC No. JAAE-23-28794; **Revised:** 24-Jan-2024, Manuscript No. JAAE-23-28794 (R); **Published:** 31-Jan-2024, DOI: 10.35248/2168-9792.23.12.327

Citation: Yakimenko OA (2024) Small Object Detection Capabilities Enabled by Employing sUAS Integrated with Modern Sensors. J Aeronaut Aerospace Eng. 12:327.

an (abandoned) small firearms on the ground but also classify them using a pretrained Convolutional Neural Network (CNN). The last example demonstrates a possible usage of a MS sensor to detect camouflaged targets and battlefield anomalies, but this time MS data were used differently by utilizing spectral indices.

LITERATURE REVIEW

Foreign object debris detection using EO sensor

The worldwide cost of dealing with Foreign Object Debris (FOD) exceeds US$13 billion per year in direct and indirect costs [3]. Even more significantly, FOD had been attributed as one of the major, if not direct, causes of several aviation crashes, the most high-profile of which was the Air France Concorde crash in July 2000 that killed 109 people on-board and four on the ground. In this particular crash, it was a piece of titanium debris, a part of a thrust reverser that had fallen from a Continental Airlines McDonnell Douglas DC-10 during takeoff about four minutes earlier. Other examples of FOD include rocks, broken pavement, ramp equipment, parts from ground vehicles, garbage, maintenance tools, bolts, lockwire, etc. (Figure 1). Airport operations, including FOD detection, place a high demand on manpower. FOD walk-downs (executed regularly on aircraft carriers) are time consuming and require significant human resources, hence are not applicable for civil airport operations. Besides, visual FOD detection by humans is found to be not reliable – in this case one piece of FOD would be found on the runway every two months, as compared to the estimated one found every two days with automated scanning.

Automation of FOD detection, proposed by Lee WL et al, provides an opportunity to improve the detection rate and productivity of manpower [4]. This research effort proposed a concept of operations of the Automated FOD Detection System (AFDS) that employs multiple small multi-rotor UAS carrying commercial-grade EO sensors to scan a runway and compare scan data with a FOD-free image library.

Small object detection algorithms were developed and validated in several flight campaigns. This research also produced a Graphical User Interface (GUI) for operating such a system (the number of drones, their speed and pattern altitude depends on the specific EO sensor to be used). This particular research used multiple commercial-of-the-shelf sUAS equipped with a typical 4K 94°-FoV EO sensor Zenmuse X3 (providing 4,000 pix by 3,000 pix resolution) flying just a few meters above the runway.

For the small square black and white FOD samples ranging in size from 2 cm to 20 cm considered in this study, Figure 2 shows the detection rate achieved during the flight testing of the developed concept/algorithms. Notably, the white FOD samples were easier to detect (due to a better contrast with the gray runway concrete/asphalt or black tire rubber marks in a touchdown zone). Figure 3 illustrates the dependance on the runway sweep pattern altitude above the ground.

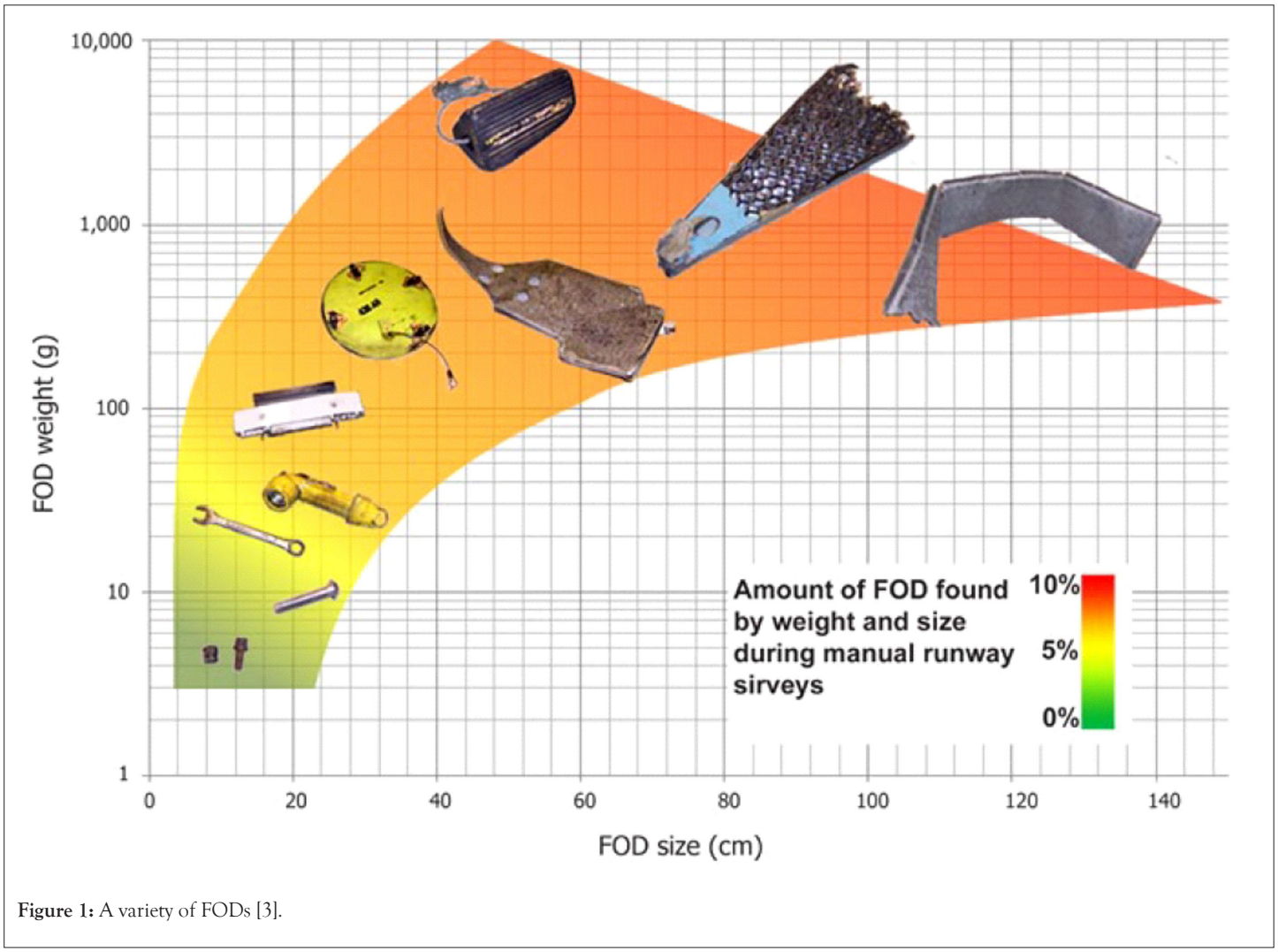

Figure 1: A variety of FODs [3].

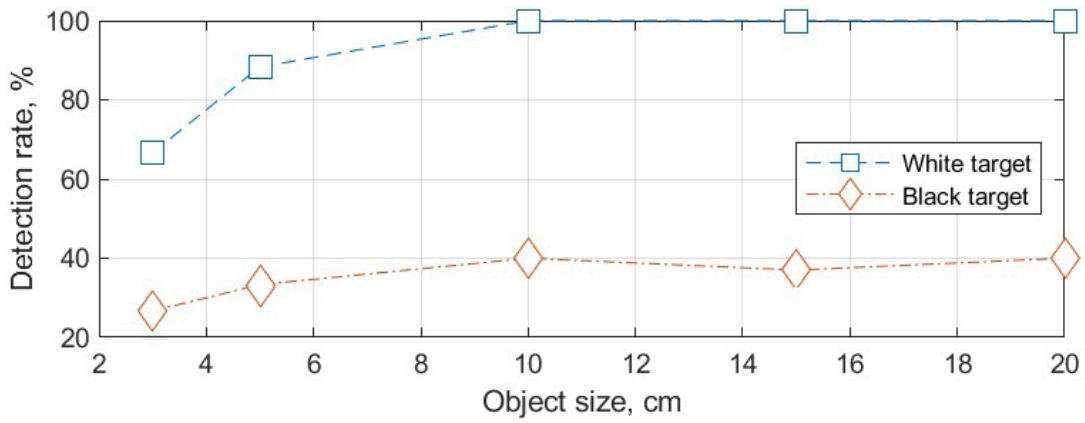

Figure 2: Detection rate of different-size black and white specimens.

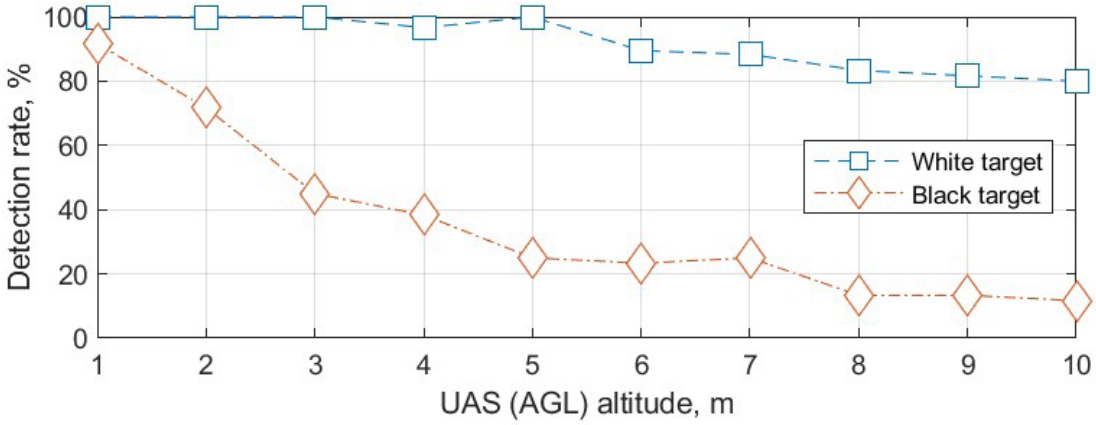

Figure 3: Detection rate versus flight altitude for black and white objects.

Planning and operation of a FOD sweep is envisioned to be conducted using a GUI shown in Figure 4. The list of detected FOD candidates for further inspection/removal shows up in the lower-right part of GUI while an operator has an opportunity to monitor the sweep using an additional GUI screen as shown in Figure 5. This specific example (Figure 4) features nine drones flying along the 46 m wide and 2 km long runway at 22 m/s 4 m above the ground. Figure 5 features the moment when the far-left drone (the first out of nine) finds a suspect FOD (denoted as a red square). In this particular case, the entire sweep took less than two minutes, which in the real-world situation would have only a negligible impact on airport operations.

This research found that the overall concept is definitely feasible with more testing needed to ensure its reliability and suitability. More sophisticated (e.g., MS) sensors can be used with FOD candidate classification added if needed.

DISCUSSION

Unexploded ordnance detection using MS sensor and ML

Unexploded ordnance is "military ammunition or explosive ordnance which has failed to function as intended" and left behind after war conflicts, weapon system testing and trainings [5]. Figure 6 shows a wide range of UXO varying by size (cf. a 155-mm projectile *vs.* a 20-mm M55 projectile), shape, and color. Clearly, UXO poses a threat to soldiers operating in mission areas, but current UXO detection systems do not necessarily provide the required safety and efficiency to protect soldiers from this hazard.

A new UXO detection system include, proposed and investigated by Cho S et al, takes advantage of employing a Deep Learning Convolutional Neural Network (DLCNN) trained to detect UXO in multiple spectral bands as recorded by MS sensor integrated with sUAS [6].

While traditional single-lens sensors combine and store visible light spectrum (400 nm-700 nm) as Red-Green-Blue images, MS sensors employ multiple lenses to capture multiple images in a selected sets of wavelength bands. The latter may include wavelengths invisible to the human eye. For example, a popular MicaSense RedEdge-MX sensor used in the UXO detection study featured five narrow bands centered around Blue (475 nm), Green (560 nm), Red (668 nm), Red Edge (RE) (717 nm), and (invisible) Near-Infrared (NIR) (840 nm) spectra [7]. As seen from Figure 7, RE spectrum (between 690 nm and 730 nm) is located in the very beginning of the non-visible light spectra in the region of rapid change in reflectance of vegetation, and as such can be very useful in detecting variations in the physical environment (e.g., disturbed soil) and in chemical properties.

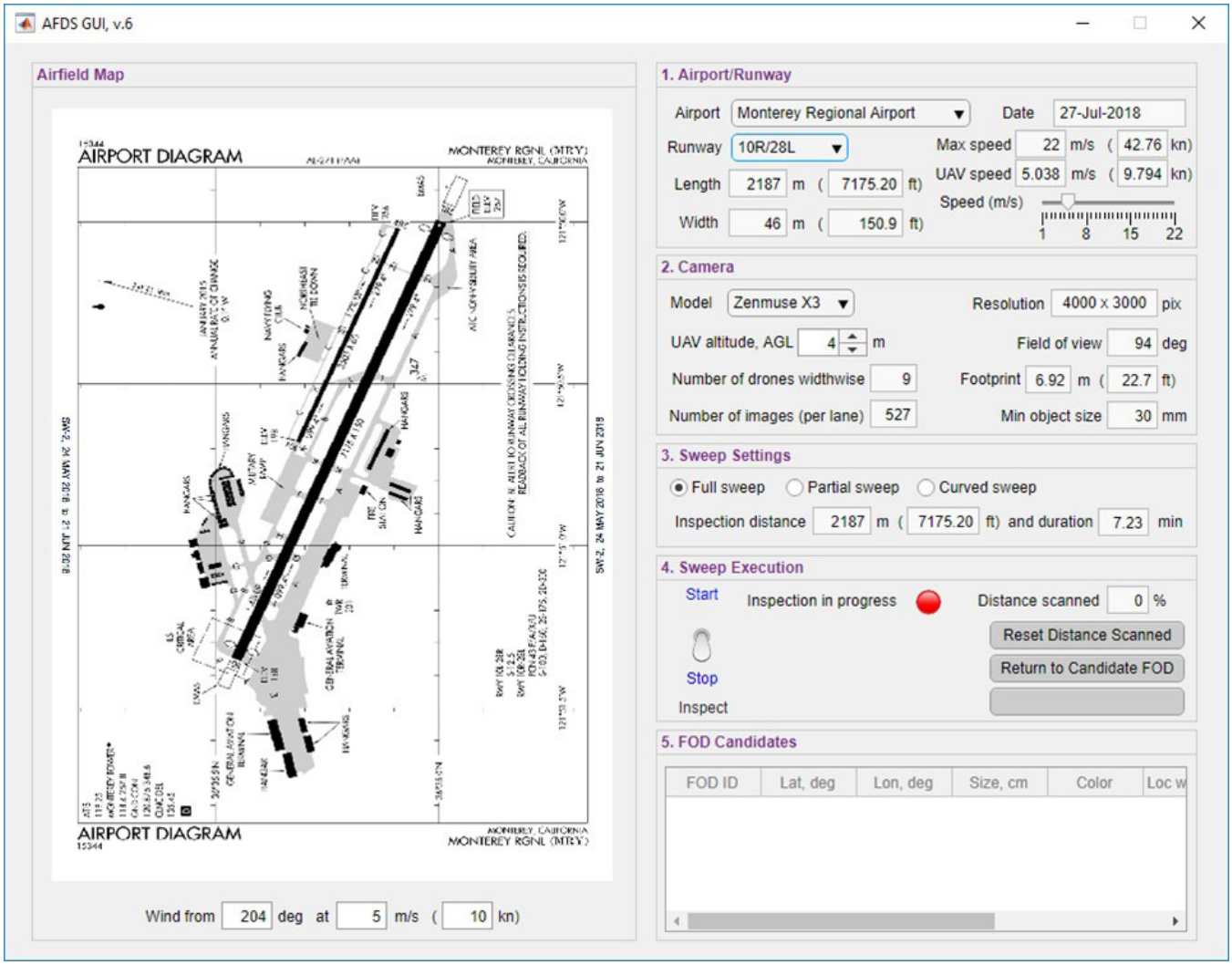

Figure 4: Prototype of AFDS GUI.

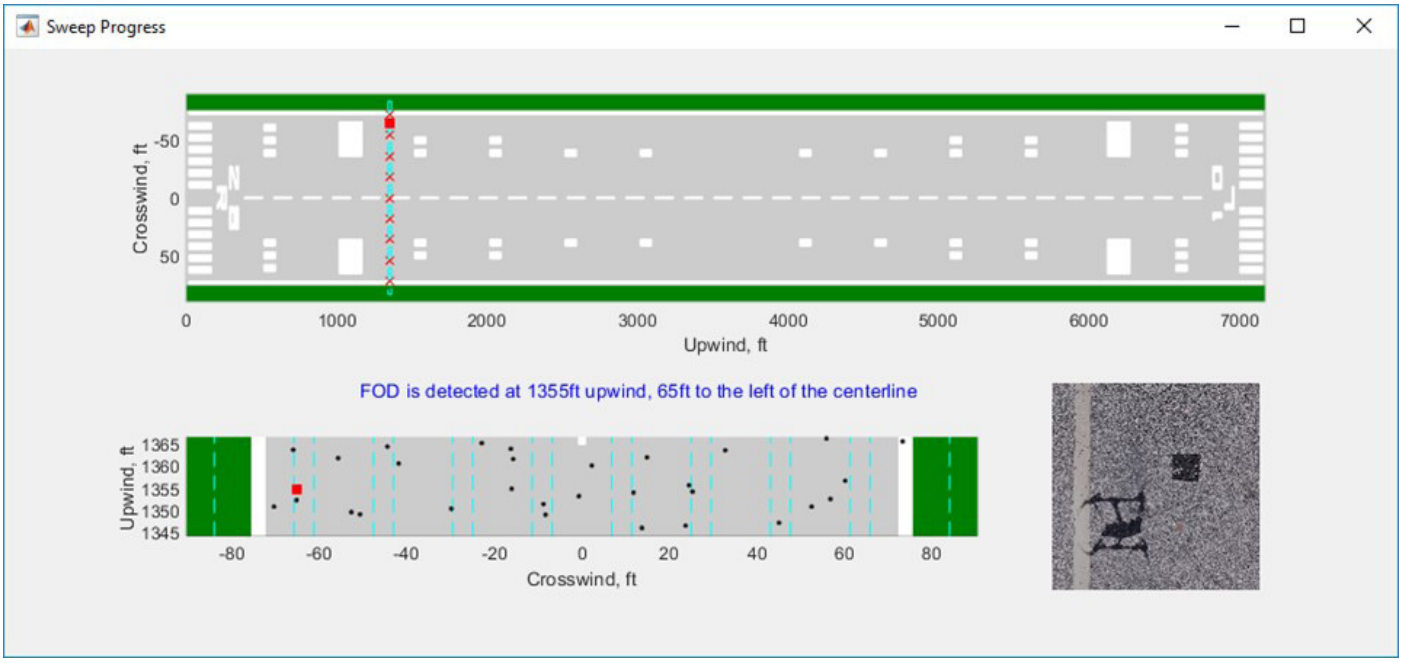

Figure 5: Detachable window showing the image of a detected FOD candidate.

Figure 6: Sample UXO found during Fort Ord ex-military base clean up.

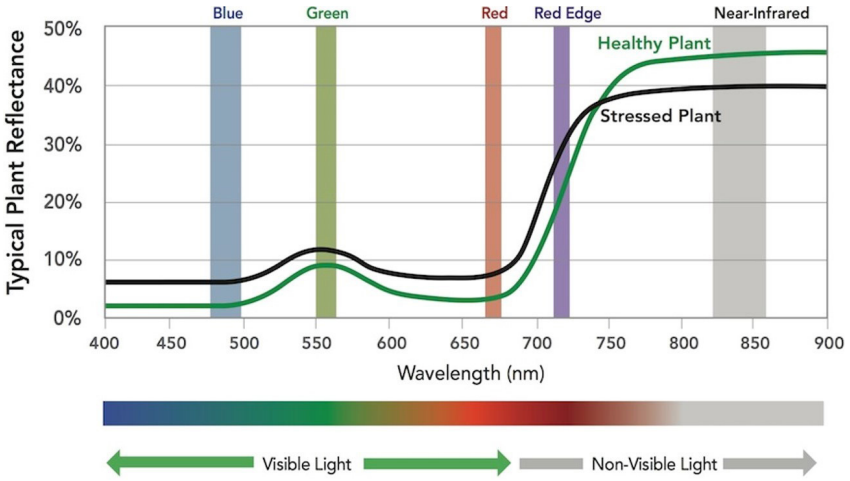

Figure 7: Spectrum bands of MicaSense RedEdge-MX sensor against spectral reflectance curve for vegetation [7].

MS sensors have already proved to be a very useful tool in agriculture, forestry and land management applications, and there is definitely a potential to contribute to detecting man-manned objects against natural background (to include soil and vegetation). Having such a sensor integrated with sUAS allows covering up to 0.3 km^2 within about 15 minutes, i.e., during a single sortie. Having multiple sUAS (as in the application described in the previous section) extends the search capability even further.

Figure 8 gives an example of five images recorded by each individual spectrum lens of MicaSense RedEdge-MX sensor. While all images look somewhat the same, there may be slightly different sets of scene features captured by each of them, thus complementing each other.

After experimenting with different CNNs, the ResNet50, a variant of ResNet model, was finally chosen for UXO detection (ResNet50 refers to the Residual Network with 50 layers based on residual learning). The developed DLCNN ends with the YOLO output layer (YOLO is the most successful object detection algorithm in the field) providing locations of the refined Bounding Boxes (BBs) enclosing all candidate UXO. Each spectrum is trained with its own DLCNN and the resulting BBs for each band are also shown in the individual spectrum images of Figure 8.

While in the particular case shown in Figure 8 the UXO was found in each individual band, in practice it is not necessarily the case. Quite often, only the blue and green detectors were successful while three other detectors were not. In some other cases, only the NIR detector detected UXO while other detectors failed. The developed two-step BB merging procedure fuses five detection results together to take advantage of having multiple bands (positive detections). Figure 9 visualizes this procedure for a specific case when only the blue and green detectors are successful. Indeed, having five opportunities to detect UXO rather than just one as provided by a single EO sensor increases the overall probability of detecting UXO.

The DLCNN detectors developed and trained on realistic imagery proved overall feasibility of the concept and demonstrated quite a promising performance. With only about 1,000 images (per each spectrum band) needed to train a single detector, it takes on the order two hours to prepare (resize, label, augment) data and about 1-2 hours to actually train the detector (in the MATLAB interpretative environment). Once trained, however, the detector can process a streamed video at the 10 fps rate. For compiled code, this rate is estimated to be at least two orders of magnitude higher.

As far as the ratio of correctly predicted positives and predicted positives, even a standard EO camera allows detecting UXO with ~0.77 Average Precision (AP). Employing a MS sensor with multiple spectrum bands, especially RE and NIR, allows capturing different sets of features so that while the AP values for the individual spectrum bands are lower than that of the EO sensor, when combined (fused) they ensure much better detection results.

Of course, to increase a Technology Readiness Level (TRL) of the developed prototype, more research needs to be conducted (for example, to tackle motion blur and occlusion), but in general finding UXO using a MS sensor proved to be a feasible approach worth further exploration.

Detection and classification of small firearms using EO sensor and ML

The research effort presented in the previous section was further expanded to explore feasibility of not only detecting different small objects using imagery collected by sUAS but also classifying them into different categories. Rather than UXO, "lost" small firearms were used as a realistic operational scenario [8]. Specifically, three classes of different shape/size/color small firearms were considered: pistol, black rifle, and brown rifle (shown in Figures 10a-10c, respectively).

This particular research used a single EO rather than a MS sensor (as was the case in the study described in the previous section). Zenmuse X5, a 16-megapixel EO RGB sensor with a video resolution of 4,096 pix by 2,160 pix and shutter speed of 1/8000 s, was integrated with sUAS. To collect imagery for CNN training, sUAS flew search patterns over a 28.7 m by 15.2 m (440 m^2) operating area. During data collection, the positions and orientations of the objects were varied.

Obviously, finding and classifying a pistol appears to be a more challenging task compared to finding the larger objects (rifles) because a smaller object can sometimes be confused with a shadow

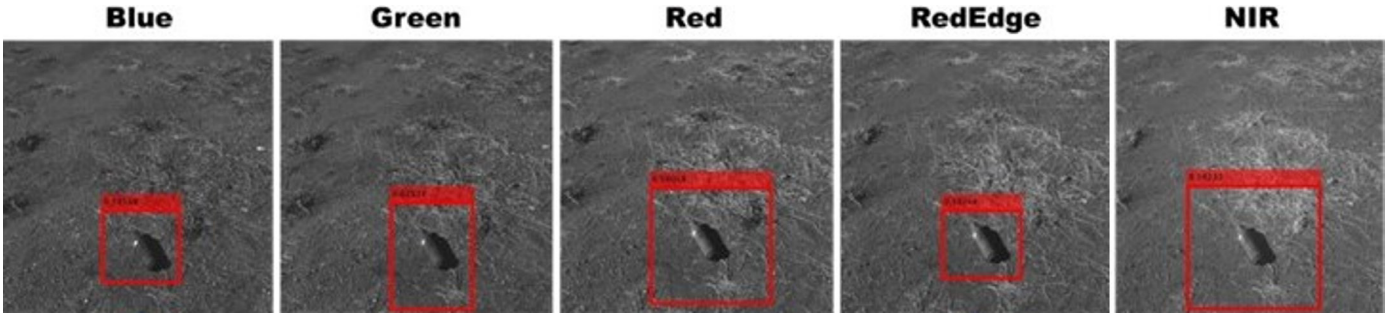

Figure 8: BBs for a detected UXO as seen on MS images.

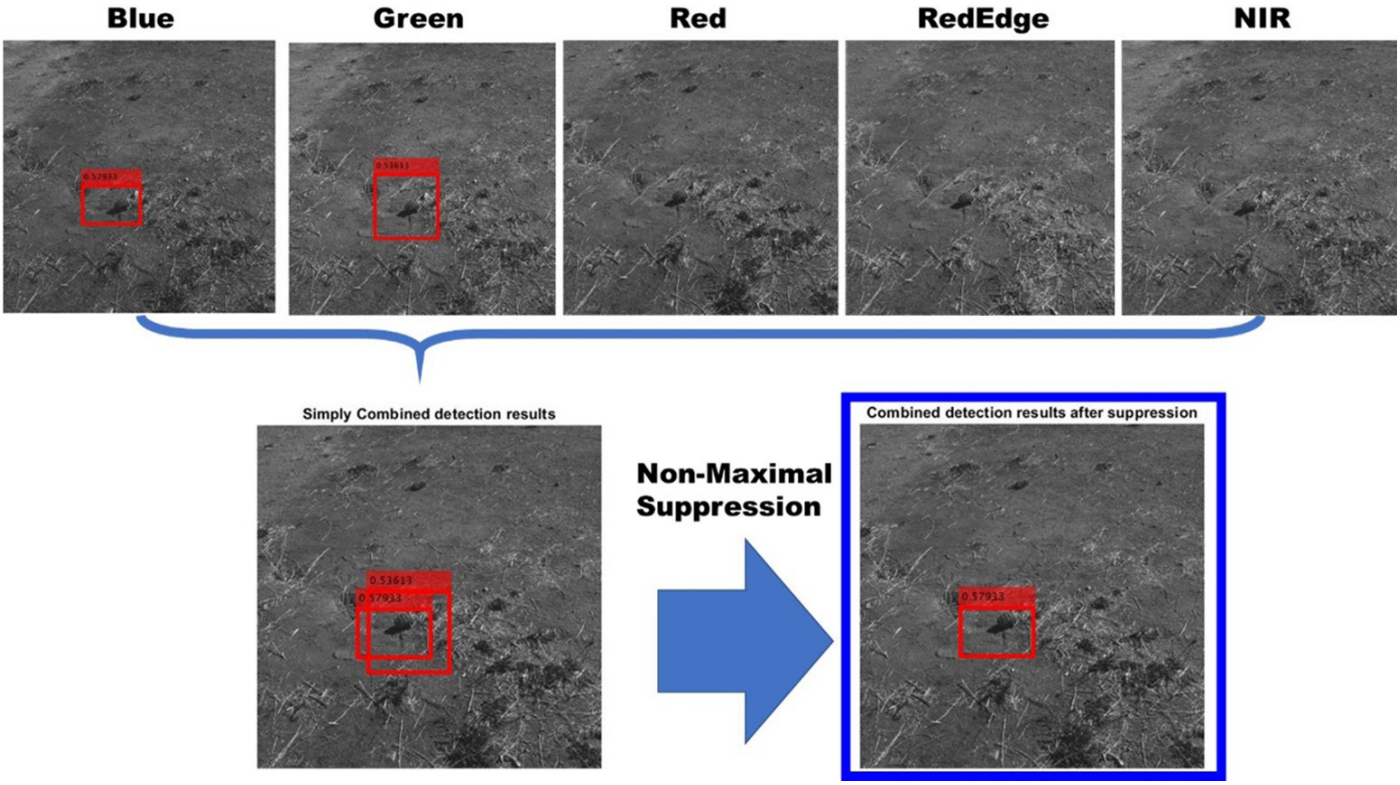

Figure 9: Results of detection in multiple spectra and the final merging BB.

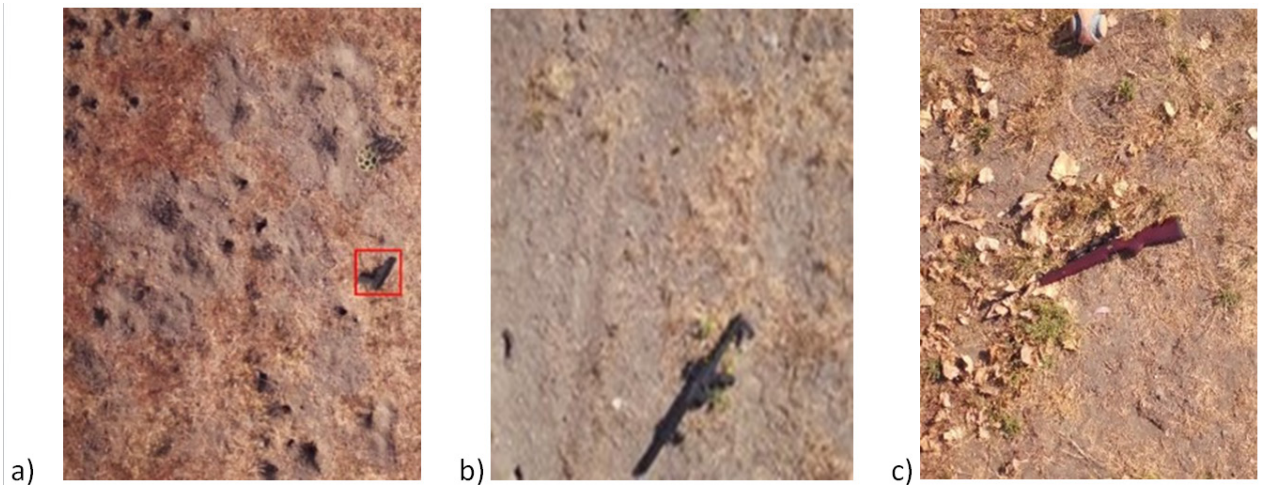

Figure 10: Objects of interest: Pistol (in red box) (a), black rifle (b), and brown rifle (c).

or black stone. The confusion may also occur when even the larger objects are partially obscured. To this end, Figure 10c illustrates an example when a brown rifle barrel is intentionally obscured by leaves.

A total of 3,140 images of small firearms were collected to train CNN. Data augmentation (resulted in a fourfold increase of the training data set) was applied to improve overall performance of proposed system. Following imagery collection and conditioning, the Faster RCNN, YOLO, and SSD models were explored to see which one delivers the best performance in detecting small firearms.

It was determined that the same YOLO model with a ResNet-50 backbone network as in the study addressed in the previous section was the most effective for small firearms detection and classification as well. The model was trained with eight anchors, (predefined BBs of a certain height and width), mini-batch size of eight, learning rate of 0.001, and maximum number of epochs of ten, which happened to be the best set of parameters. The training time happened to be about 1 hr and 20 min for each run. The trained network demonstrated very good results featuring a mean AP (mAP) of 0.97 (0.98-for the good-contrast objects regardless of their size, and 0.94-for a lower-contrast objects). Good performance was demonstrated even for the partially occluded objects (see examples in Figures 11a-11c). Obviously, tuning CNN for the best performance requires additional efforts. To this end, several experiments were conducted with varying the aforementioned CNN parameters. As expected, the learning rate (that controls how much to change the model in response to the estimated error each time the model weights are updated) and the number of anchors, happened to be the most important parameters. For example, when the learning rate was increased from 0.001 to 0.01, the mAP dropped to almost 0, and when the number of anchor boxes was increased from eight to eleven, mAP changed to 0.95 (1 for the pistol and brown rifle, and 0.95 for a black rifle).

A high probability of correct detection/classification proves that such a system can be developed, prototyped and tested in a realistic operational environment which is the direction of the follow-up research. For the small firearm detection mission, the multirotor sUAS would fly a pattern maintaining a fixed ~3 m height above the ground level at a constant speed of ~1.4 m/s. In this case, during a 30 min flight, a single sUAS could cover on the order of 1,300 m^2. Another direction of the future research efforts is exploring different ways of augmenting existing (limited) data sets by applying various rendering effects and varying background complexity. Also, it would be interesting to quantify how the shape, size, and orientation of anchor boxes affect the performance of detectors.

Detection of camouflaged targets and battlefield anomalies using spectral indices

In response to the extended usage of tactical- and theater-level UAS for reconnaissance and surveillance in the modern battlefield, the ground forces put more and more emphasize on hiding their assets using camouflage or exploiting terrain and vegetation. In their research, Barmpas S et al used a more advanced version of the MicaSence sensor, MicaSence RedEdge-P, featuring five-band MS and panchromatic sensors to explore capability of defeating camouflage and still detecting battlefield anomalies that otherwise are not visible using regular daytime/nighttime vision sensors [9].

Figures 12a-12c illustrates examples of uncamouflaged and camouflaged targets used in this study as well as an example of battlefield anomalies, like a landmine or Improvised Explosive Device (IED), that can potentially be recognized by disturbed soil.

The results of the extensive flight campaign were evaluated using two criteria. The first criterion was the ability to detect the target by employing different spectral indices. The second criterion examined the ability of MS sensor to provide a better detection compared to a regular EO or panchromatic sensor (the former one creates a complete three-color image, while the latter produces a single-band grayscale image that combines the information from the visible red, green, and blue bands).

A spectral index is a mathematical equation that is applied to the various spectral bands for each pixel. This research studied a variety of well-established indices blending two different spectra that are commonly used in agriculture to enhance vegetation and more specifically healthy vegetation. However, neither of them worked to defeat camouflage. Then, target reflection in each individual spectrum was examined against different backgrounds to include grass, tree, tree shadow, and grass under a tree (Figure 13).

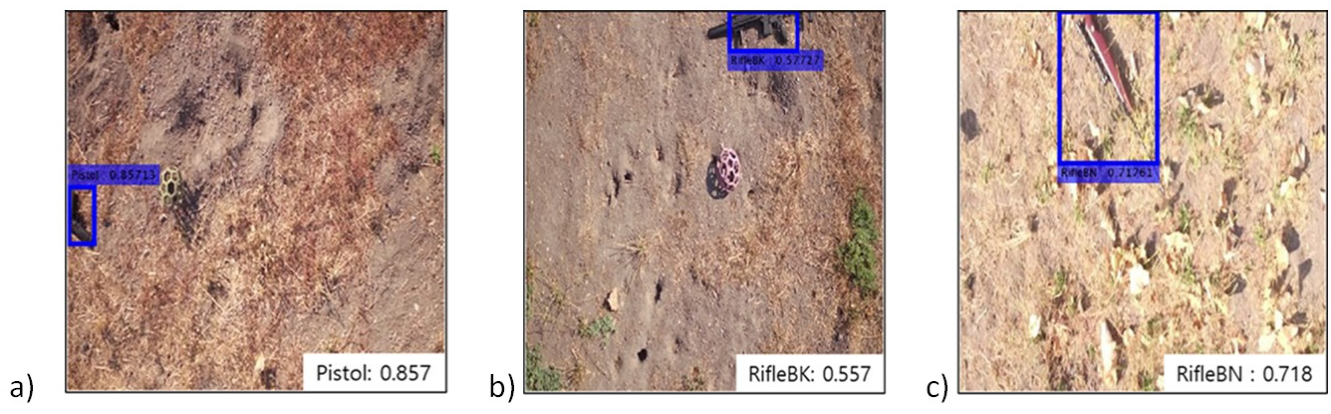

Figure 11: Detection of partially occluded pistol (a), black rifle (b), and brown rifle (c).

Figure 12: Examples of the objects to detect: open-terrain target (a), camouflaged target (b), buried IED (c).

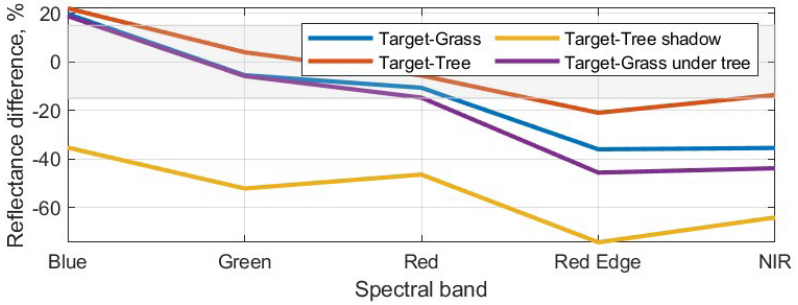

Figure 13: Difference of spectral reflectance of target *vs.* Underlying environment in different bands.

The RE band exhibited the largest (negative) difference for all examined environments (NIR would be another alternative). The blue band exhibited some (positive) differences and a relatively large negative difference for a tree shadow environment. Hence, combining these two bands into the spectral index NDREBI=(RE-Blue)/(RE+Blue) ensured the best result.

In the case of detecting the freshly buried objects simulating landmines and IEDs, it was the NDVI index, NDVI= (NIR-RED)/(NIR+RED), that provided the better detection results compared to NDREBI due to its ability to distinguish disturbed soil from vegetation or undisturbed soil.

Figures 14-16 illustrate effectiveness of using these two spectral indices when flying a MS sensor at a relatively high (for sUAS) altitudes of 50 m to 100 m. Specifically, Figures 13a and 13b show the cropped NDREBI images with an open terrain uncamouflaged and camouflaged targets (both clearly identifiable) when flying at 100 m above the ground.

Even when placed under a tree, the NDREBI image is still useful for finding the target (Figures 14a and 14b). Obviously, the lower altitude the better detection capability is.

Figures 15 and 16 illustrate NDVI capability to detect disturbed soil (relative to detection of the two targets shown in Figure 12c).

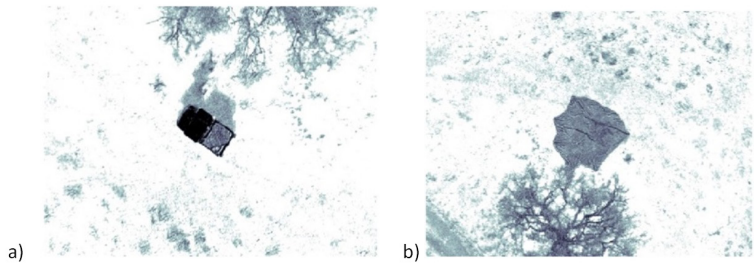

Figure 14: NDREBI images of the target out in the open terrain without (a) and with (b) camouflage for a 100 m AGL flight.

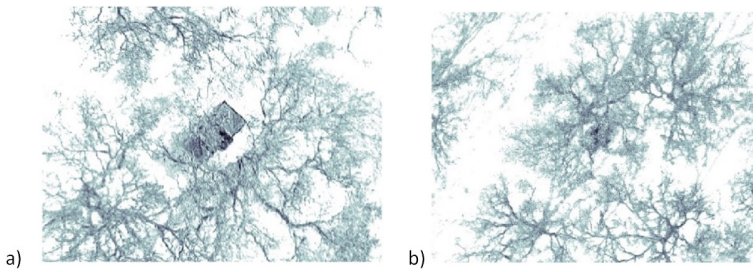

Figure 15: NDREBI images of the uncamouflaged target partially obscured by trees for the 50 m AGL (a) and 100 m AGL (b) flight patterns.

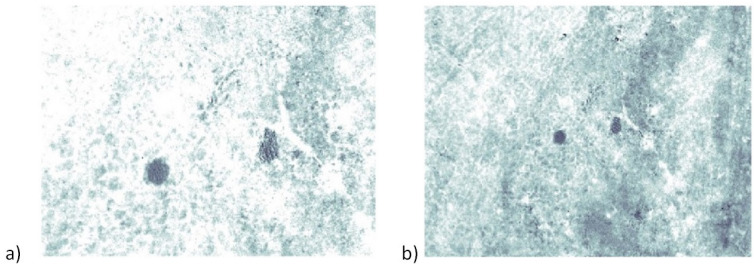

Figure 16: NDVI images of the target for the 50 m AGL (a) and 100 m AGL (b) flight patterns.

CONCLUSION

This paper provided a brief review of several research efforts aimed at finding new applications for sUAS integrated with EO/MS sensors and empowered by using the ML algorithms. This includes using single and multiple sUAS to detect (and classify) foreign object debris on a runway; unexploded ordnance; small firearms; camouflaged targets and battlefield anomalies. The developed detection algorithms have been tested in real flight campaigns and are mature enough to be advanced to the higher TRLs. While these algorithms were specifically targeting the small objects, they can easily be scaled up and applied to find larger objects while utilizing bigger UAS flying at higher altitudes and utilizing different sensors (e.g., see the current research effort in [10]).

REFERENCES

1. Wescam mx-series airborne surveillance solutions, L3Harris Technologies
2. Available cameras for trinity f90+, Quantum Systems
3. Mccreary I, Runway safety: FOD, birds, and the case for automated scanning. Insight SRI. 2010:146-57.
4. Lee WL, Yakimenko O. Feasibility assessment of sUAS-based automated FOD detection system. ICCR. 2018:89-97.
5. Martin MF, Dolven B, Feickert A, Lum T. War legacy issues in southeast asia: Unexploded Ordnance (UXO). Current Politics and Economics of South, Southeastern, and Central Asia. 2019;28(2/3):199-230.
6. Cho S, Ma J, Yakimenko OA. Aerial multi-spectral AI-based detection system for unexploded ordnance. Defence Technology. 2023;27:24-37.
7. MicaSense RedEdge, Micasense, 2022 20:58.
8. Ma J, Yakimenko OA. The concept of sUAS/DL-based system for detecting and classifying abandoned small firearms. Defence Technology. 2023;30:23-31.
9. Barmpas S, Yakimenko, O.A. "Using aerial multispectral imaging to detect man-made anomalies," to appear in the proceedings of 34th congress of the international council of the aeronautical sciences, Florence, Italy, 2024.
10. Donaldson TQ, von Flotow A, John S, Goff J, Yakimenko O, Brodie R, et al. Improve ocean sensing using unmanned aerial vehicles. Mar. Technol. Soc. J 2023;57(4):47-51.